AJP-Cell Articles in PresS. Published on May 15, 2002 as DOI 10.1152/ajpcell.00159.2002

Functional studies of the kidney of living animals using multicolor 2-photon microscopy

Kenneth W. Dunn*, Ruben M. Sandoval*, Katherine J. Kelly*, Pierre C. Dagher*, George A. Tanner[#], Simon J. Atkinson*, Robert L. Bacallao*^, Bruce A. Molitoris*^

* Department of Medicine, Division of Nephrology, Indiana Center for Biological Microscopy, ^Roudebush Veteran's Administration Medical Center, [#]Department of Cellular and Integrative Physiology, Indiana University Medical Center, Indianapolis, IN 46202

Correspondence should be sent to:

Kenneth Dunn
Department of Medicine
Division of Nephrology
Indiana University Medical Center
1120 South Dr., FH 115
Indianapolis, IN 46202

Telephone: 317-278-0436
FAX: 317-274-8575
Email: kwdunn@iupui.edu

Running title: Intravital 2-photon microscopy of kidney

Key words: fluorescence, microscopy, 2-photon, multiphoton, in vivo, intravital, kidney

ABSTRACT

Optical microscopy, when applied to living animals, provides a powerful means of studying cell biology in the most physiologically relevant setting. The ability of 2-photon microscopy to collect optical sections deep into biological tissues has opened up the field of intravital microscopy to high-resolution studies of the brain, lens, skin and tumors. Here we present examples of how 2-photon microscopy can be applied to intravital studies of kidney physiology. As the kidney is easily externalized without compromising its function, microscopy can be used to evaluate various aspects of renal function *in vivo.* These include cell vitality and apoptosis, fluid transport, receptor-mediated endocytosis, blood flow and leukocyte trafficking. Efficient 2-photon excitation of multiple fluorophores permits comparison of multiple probes and simultaneous characterization of multiple parameters, and yields spectral information that is crucial to the interpretation of images containing uncharacterized autofluorescence. The studies described here demonstrate how 2-photon microscopy can provide a level of resolution previously unattainable in intravital microscopy, enabling kinetic analyses and physiological studies of the organs of living animals with subcellular resolution.

INTRODUCTION

Fluorescence microscopy has become an invaluable tool in biomedical research. The power of fluorescence microscopy has recently been extended by a unique combination of technical developments in fluorescent probe technology, photonics and optics. Specific probes may be conjugated to newly-developed fluorophores that span the spectrum of light, allowing the subcellular distribution of multiple molecules to be compared. New fluorescent probes, sensitive to a variety of physical parameters, permit quantitative physiological studies to be conducted within individual cells. New color variants of the Green Fluorescent Protein (GFP) have been developed, providing researchers with the ability to compare the behaviors of multiple, endogenously expressed proteins within living cells and tissues.

The development of faster and more sensitive imaging systems has been instrumental to the rapid growth in studies of living cells. Studies of living cells not only permit evaluations of cell physiology and molecular dynamics, they also provide morphological data that is unaffected by questions of cell preservation. Studies of living cells have largely been limited to model systems: cultured cells, isolated primary cells or freshly isolated tissue segments. It is always a concern that these experimental systems, while experimentally tractable, may not accurately represent the *in vivo* situation because they generally lack interactions with the supporting tissues, including the vasculature, nervous system and extracellular matrix. In the end, the most meaningful behaviors of cells will be observed in living animals.

Unlike in vitro preparations, the thickness of intravital microscopy samples presents the microscope with a challenging optical situation where out-of-focus blur and light scattering combine to compromise image resolution and contrast. The quality of microscopic images of thick tissues is improved by confocal microscopy, which rejects out-of-focus light. However, the aperture that

provides optical sectioning also rejects scattered fluorescence from the in-focus plane, so that confocal microscopy is capable of collecting images only tens of microns into biological tissues.

The recent development of 2-photon microscopy (9, 10) has provided researchers with the means to collect high-resolution optical sections deep into biological tissues. Since 2-photon fluorescence depends upon the simultaneous absorption of two photons of light, fluorescence excitation occurs only at the focal point, where the density of illuminating photons is highest. Since no out-of-focus fluorescence is generated, fluorescence may be collected without a confocal aperture, thus increasing the ability to collect the fluorescence generated deep into light scattering biological samples (5). The extended reach of 2-photon microscopy has been applied to intravital studies of the morphology and physiology of the brain (6, 14, 19, 23, 37, 38), the metabolism of skin (25), the development and vascularization of tumors (2) and embryonic development (35).

Here we present examples of how 2-photon microscopy can be applied to intravital studies of kidney physiology and pathophysiology. Because of its intimate relationship to the vasculature, the kidney may be readily labeled by intravenous injection of fluorescent probes. As the kidney is easily externalized without compromising its function, microscopy may be used to evaluate a variety of renal parameters. Previous intravital studies of the kidney have used conventional fluorescence, reflected light, and transillumination microscopy to study organic anion transport (36, 40), tubular obstruction (41) and the microcirculation and tubular fluid flow (12, 15, 42).

Two-photon microscopy offers significant advantages for physiological studies of the kidney. First, it provides high resolution, sufficient to characterize subcellular structures and events. Second, the extended optical sectioning of 2-photon microscopy provides true 3-dimensional information that is critical to interpreting the complex organization of the kidney (30). Our studies have identified a range of interesting and powerful new applications for intravital imaging of the kidney by multi-photon

microscopy. These studies demonstrate that multiple fluorophores can be simultaneously excited by 2-photon absorption, allowing comparison of multiple probes and simultaneous characterization of multiple parameters. This spectral information is also crucial to interpreting images containing uncharacterized autofluorescence.

MATERIALS AND METHODS

Animal Models

All animal studies were conducted in conformity with the National Institutes of Health Guide for the Care and Use of Laboratory Animals. Male Munich-Wistar and Sprague-Dawley rats (200-250 g body weight), male control and Tie-2-GFP mice (26) at 8-10 weeks of age and heterozygous adult male Han:SPRD rats with autosomal dominant polycystic kidney disease (34, 40) were used as described below. Animals were anesthetized using thiobutabarbital (Inactin) ~ 130 mg/kg body weight i.p. (Sigma, St. Louis, MO). After assuring adequate anesthesia, a 10-15 mm lateral incision was made dorsally under sterile conditions. The kidney was exteriorized and a 27 gauge (for rat) or 30 gauge (for mouse) cannula was then inserted into the tail vein for dye infusion. For studies in which ischemia was induced, the renal artery and vein were occluded with a non-traumatic microaneurysm clamp for 30 minutes. For studies in which the medullary region of the rat or mouse was imaged, a parenchymal window was cut through the avascular plane of the kidney. During all procedures, core body temperature was maintained using a homeothermic table.

Fluorescent Probes

Fluorescent probes were dissolved in isotonic saline and injected into rats in a 0.5-1.0 ml bolus over approximately 3 minutes. The total volume injected into mice was approximately 0.2 ml. The probes used in this study are summarized in Table 1, which also lists the amounts injected for each probe. Except as noted, imaging commenced within 5 minutes of injection. All probes were obtained from Molecular Probes (Eugene, OR).

Micropuncture Procedure

Micropuncture studies were conducted as described before (39). Briefly, the anesthetized rat was placed on a heated animal board and rectal temperature was monitored with a probe and kept at 37°C. Surgical procedures included a tracheostomy, cannulation of femoral artery and vein, and placement of the left kidney in a micropuncture cup. During surgery the rat was given 1 ml of a 6 g/100 ml bovine serum albumin solution in 0.9% NaCl, and this was followed by a constant intravenous infusion of isotonic saline at 3 ml/hr. Micropuncture was accomplished at 100X magnification using a Leitz stereoscopic microscope. Proximal tubule lumens were punctured with sharpened 7-8 μm tip diameter pipettes using a Leitz micromanipulator. Solutions were slowly infused into tubules by applying pressure to the micropipette contents with a mercury leveling bulb. The solutions were colored with 100 mg/dl lissamine green to observe fluid flow. Sudan black-stained castor oil was injected into nearby nephrons to aid in subsequent localization of the infused tubules. A careful drawing was made of the infused tubules in relation to tubules containing oil. The animal was transported to the stage of the two-photon microscope, the labeled nephrons were identified, and images were collected.

Microscopy

All imaging was conducted using a Bio-Rad MRC-1024MP Laser Scanning Confocal/Multiphoton Scanner (Hercules, CA) attached to a Nikon Diaphot inverted microscope (Fryer Co, Huntley, IL) using a Nikon 60X NA 1.2 water-immersion objective. Fluorescence excitation was provided by a Titanium-Sapphire laser (Spectraphysics, Mountain View, CA). After evaluating a range of excitation wavelengths, the best results for stimulating fluorescence in triply labeled samples were obtained using 800 nm excitation, which was used for all studies. Laser output

was attenuated with neutral density filters to between 3% and 40% so that, after accounting for losses in the optical train of the microscope, we estimate that the power at the surface of the kidney was between 2 and 28 mw. Power at the focal point is harder to estimate due to absorption by the tissue, but will be lower than these values, depending upon the depth of imaging.

A water circulating heating pad was placed on the stage approximately 1 hour before image acquisition took place to heat the stage to 37ºC. Animals were placed on the stage with the exposed kidney placed in a 50 mm diameter coverslip-bottomed cell culture dish (Warner Inst., Hamden, CT) bathed in isotonic saline (Figure 1). The coverslip-bottomed dish was secured to the stage plate by applying adhesive tape to the bottom of the dish. To minimize motion, the animal was placed so the kidney was as close to the edge of the dish as possible, placing the chest outside the dish to minimize movement of the kidney during image acquisition. The heating pad was then placed directly over the animal and supplemental oxygen was provided. Due to animal movement and respiration, images were collected rapidly in a single scan at either the "fast" or "normal" speed setting (providing acquisitions in approximately 0.5 and 1 second, respectively).

Image processing

In some cases, the noise inherent in the rapidly-acquired images was reduced by applying a 3x3 low-pass filter to each image, using Metamorph Image Processing Software (Universal Imaging, West Chester, PA). Final preparation of images, including adjustments in brightness and contrast, was conducted using Adobe Photoshop (Adobe, Mountain View, CA).

Rotated volume renderings were produced using Voxx volume rendering software developed by the Indiana Center for Biological Microscopy (7). The real-time renderings produced using Voxx were then recorded as movies using Adobe Premiere (Adobe, Mountain View, CA), which was also

used to produce the time series movies. Palette mapping functions in Voxx software were also used to enhance the contrast of rendered volumes.

Although the colors shown in the figures are similar to the "true" colors of probe fluorescence, they are digital reconstructions. As discussed above, 800 nm illumination stimulates a broad spectrum of fluorescence in triply-labeled samples. This spectrum of fluorescence is split into three channels, centered at 605 nm, 525 nm and 455 nm, which are then collected in separate photomultiplier tube detectors. These three channels, displayed as pure red, green and blue respectively, are then recombined in the color figures. In some cases, the contrast and brightness of each color was further adjusted for clarity.

As the photomultiplier tubes were adjusted differently for each experiment, the hue of specific objects in the images varies slightly between experiments. For example, the brown autofluorescent inclusions of proximal tubule cells (discussed below) may appear more reddish or yellowish, depending upon how the photomultiplier settings for the "red" and "green" channels are adjusted.

RESULTS

DNA stains can be used as intravital labels of cell nuclei in the kidney and to identify necrotic or apoptotic cells. Examples of intravital imaging of the kidneys of rats injected with Hoechst 33342 and propidium iodide are shown in Figure 2. Hoechst 33342, a cell-permeant DNA-binding dye is rapidly distributed throughout the kidney following tail-vein injection, and brightly labels nuclei of the endothelia, circulating leukocytes, the glomerulus, interstitial cells, and the different renal epithelial cells. Propidium iodide is a membrane-impermeant DNA-binding probe that is excluded from living cells, and can thus be used to identify dead or dying cells with a compromised plasma membrane. By injecting an animal with both probes, one can determine the fraction of necrotic cells in a tissue from the proportion of nuclei labeled with Hoechst that are also labeled with propidium iodide (identified by the white fluorescence that results from the combined contributions of blue Hoechst and orange propidium iodide fluorescence).

Figure 2A shows a projection of a 50-micron-thick volume collected from the superficial cortex of the kidney of a control animal, whereas Figure 2B shows the projection of a similar volume collected from an animal following 30 minutes of renal ischemia and 24 hours of reperfusion. These volumes are better evaluated as animations of volume renderings, presented at "http://www.nephrology.iupui.edu/dunnetal". Whereas the control kidney showed no evidence of dead cells, the post-ischemic kidney contained numerous dead cells, with nuclei labeled with both dyes. In both cases, proximal tubules were found to contain punctate structures with an endogenous brown autofluorescence. In the post-ischemic kidney, brown autofluorescence was also observed in what appear to be protein casts in the tubule lumens.

The working distance of the Nikon 60X water immersion objective limits imaging depth to 200 microns into kidney tissues. Using Munich-Wistar rats, this distance is sufficient to image proximal tubules, distal tubules and superficial glomeruli in intact kidneys placed on the microscope coverglass. Preparation of a posterior parenchymal window allowed imaging of the medulla. A comparison of cell death in the cortex and the medulla following ischemia is shown in Figures 2C and D, respectively. These images show that, consistent with previous studies (18), ischemia more severely affects the medulla, which was littered with numerous dead cells in both the walls of the tubules and in the cellular debris of the tubule lumens.

The ability to collect three colors of fluorescence was key to the interpretation of these studies, allowing distinction of four types of cells (Figure 2D). Viable cells are identified by their intact nuclei that lack propidium iodide labeling. The nuclei of necrotic cells are similar in morphology, but are accessible to propidium iodide (large arrows). Cells in the early stages of apoptosis, whose plasma membrane is still intact, can be identified by their characteristically fragmented and condensed nuclei that are nonetheless inaccessible to propidium iodide (small arrows). As the plasma membrane integrity of apoptotic cells is lost as they progress into secondary necrosis, these fragmented nuclei become increasingly labeled with propidium iodide (arrowheads)

Finally, the punctate autofluorescent structures of the proximal tubule cells could be easily distinguished by their characteristic fluorescent signature. Color imaging was thus crucial to identifying DNA fluorescence, particularly after ischemia, when fragmented nuclei are frequently similar in size and shape to the autofluorescent structures, but distinct in color.

Bulk fluid-phase probes can be used to evaluate renal fluid dynamics intravitally. Intravital fluorescence microscopy has been used to assess blood flow in the liver (8, 43), brain (17), bone (46) and developing tumors (44). Similar studies of the kidney have largely used a split hydronephrotic rat

kidney model, in which tubular atrophy results in a thin tissue preparation suitable for wide-field transillumination microscopy (4, 12). In the interest of developing an experimental system that better models urinary flow, Heuser et al. (15) used epifluorescence microscopy to evaluate cortical blood flow in normal kidneys. Recently, Brown et al. (2) demonstrated the value of multi-photon microscopy in a study of blood flow deep into intradermal tumors.

We have used multi-color 2-photon microscopy of animals injected with fluid phase probes to characterize bulk fluid flow through the kidney of living animals. As outlined below, these studies demonstrate how bulk tracers may be used to assess capillary blood flow, glomerular filtration, fluid transport and tubular solute concentration. In addition, the bulk tracer dextran can be used to characterize endocytosis by proximal tubule cells (22).

Figure 3A shows a microscope field collected from the kidney of a rat that had been injected with a combination of Hoechst 33342, rhodamine-conjugated albumin and 10,000 MW fluorescein-conjugated dextran. The blue Hoechst fluorescence labeled the nuclei of all cells in the field. The red fluorescence of the albumin conjugate was limited to the capillaries in this field, whereas the small dextran was freely filtered into the tubule lumens. The filtered green dextran was then internalized into punctate endosomes by proximal tubule cells. This image is a single frame from a series of images collected over approximately 20 seconds. This time series is shown in the animation located at "http://www.nephrology.iupui.edu/dunnetal". Circulating blood cells, which exclude the rhodamine albumin, appear as moving shadows in this animation. Significant heterogeneity in blood flow can be seen in this field, as reflected by the elongated shadows of blood cells in regions of high flow, and the nearly normal profiles of blood cells in regions of lower flow.

A similar preparation is shown in Figure 3B, which shows a field collected from an animal that had been injected with a combination of Hoechst 33342 and a 500,000 MW fluorescein conjugated

dextran. The large dextran was not filtered by the glomerulus, but remained in the vasculature, labeling the peritubular and glomerular capillaries. The 30 second time series, from which this image was selected is shown at "http://www.nephrology.iupui.edu/dunnetal". As above, blood flow through this field was highly variable, with regions of high and low flow characterized by blood cell profiles that are long or short, respectively. The punctate brown autofluorescence of proximal tubule cells is especially obvious in this field.

These preparations can also be evaluated over time to track the progress of a small molecule from the blood, across the glomerulus, to proximal tubules and then to the distal tubules. Figure 3C shows an example of an optical section of a rat kidney 14 minutes after injection of Hoechst 33342, 500,000 MW fluorescein conjugated dextran and 10,000 MW rhodamine dextran. The large green dextran is limited to peritubular capillaries, but the small dextran is filtered by the glomeruli into the renal tubules. At this time point, the small red dextran is found at moderate levels in the lumen of the proximal tubule, identified by their endocytic uptake of the red probe, and at very high concentrations in the lumen of distal tubules. A similar field, shown in Figure 3D, shows that after another 11 minutes, the red dextran has largely cleared from the lumen of the proximal tubule, and is now concentrated in the lumen of distal tubules. The characteristic avid endocytosis of the proximal tubule epithelium is reflected in the bright punctate accumulation of the filtered red dextran in endosomes in cells of the proximal tubule. Such uptake was not observed in cells of the distal tubule. Unlike most other specimens, this particular rat showed a striking lack of punctate autofluorescence. While we are interested in cultivating this characteristic in experimental animals, we have been unable to reproducibly reduce proximal tubule autofluorescence.

Similar results were obtained in studies of mice. Figure 3E shows an optical section from a mouse that had been injected with 500,000 MW fluorescein conjugated dextran and 10,000 MW

rhodamine dextran. As in rats, the large dextran was retained in the vasculature, while the small dextran was rapidly filtered into the renal tubules, accumulated in endosomes of the proximal tubule, and was concentrated in the lumen of distal tubules.

Phillips et al. (30) used 3-dimensional 2-photon imaging to evaluate the distended morphology of renal tubules in fixed tissue from a mouse model of polycystic kidney disease. We used intravital imaging to characterize the tubular morphology of the heterozygous Han:SPRD rat model of polycystic kidney disease (34, 40). Figure 3F shows a projection of a 90µm-deep volume of the kidney of an animal that had been injected with Hoechst 33342 and 10,000 MW rhodamine dextran. This volume is better appreciated in the animated rendering shown at "http://www.nephrology.iupui.edu/dunnetal". The filtered red dextran clearly delineated the characteristic distended morphology of the tubules of this animal, a morphology very similar to that observed in the mouse model characterized by Phillips et al. (30). The rapid appearance of the dextran in this cystic structure also demonstrates that this cyst was connected to a functioning glomerulus. The aberrant morphology shown in this figure is especially obvious when compared with Figure 3D, which is presented at the same magnification.

The filtration and receptor-mediated endocytosis of the aminoglycoside gentamicin can be followed over time. As demonstrated above, we see significant non-specific uptake of fluorescent dextrans by the proximal tubule epithelium. We have also evaluated the process of receptor-mediated endocytosis by proximal tubule cells, taking advantage of the megalin-mediated endocytic uptake of aminoglycoside antibiotics. Figure 4A shows a high magnification image of the kidney of a rat that had been injected 11 minutes earlier with a Texas Red conjugate of the aminoglycoside gentamicin. This fluorescent conjugate has been extensively characterized by our laboratory and has been instrumental in delineating a novel pathway of aminoglycoside trafficking from the surface membrane

directly to the Golgi complex (32,33). The fluorescent gentamicin can be seen in the lumen of a proximal tubule in the center of the image, and accumulated in brightly labeled punctate endosomes at the apices of the proximal tubule epithelium. In this case, the proximal tubule can be identified not only by its endocytic uptake, but also by the brown autofluorescent inclusions located basally in each cell. Close examination of this image also shows fluorescent gentamicin in the lumen of a distal tubule segment (top left), and in two capillaries running diagonally from bottom left to top right.

Transit of intravenously injected Texas Red-gentamicin from the blood to the proximal tubule and to the distal tubule occurs very rapidly following tail vein injection. One minute after injection, gentamicin was largely found in blood vessels, but had already accessed the lumens of proximal tubules (Figure 4B). Within 3 minutes, gentamicin had begun to clear from proximal tubule segments and to accumulate in the lumens of distal tubules, which can be identified by the lack of punctate cellular autofluorescence (Figure 4C). Comparison of this image with an image of the same field collected one minute later (Figure 4D) showed that during this minute, the bolus of gentamicin had reached a distal tubule segment previously lacking probe (bottom left of figure) and had started to strongly accumulate in another segment at the top right of the field.

Although only a single fluorescent probe was used in these studies, the ability to collect multi-color images was again critical to these studies. The characteristic color signature of the punctate autofluorescence facilitated identifying proximal tubule cells, and also clearly distinguished the autofluorescent bodies from Texas Red-gentamicin-labeled endosomes.

Fluorescent indicators can be used to evaluate vitality of individual cells within animals. In Figure 4A we showed an example of the use of 2-photon microscopy to collect high-resolution images of individual endosomes within the cells of a living animal. As with cultured cells, cell-permeant probes can be used to label intracellular compartments in living animals. Rhodamine 6G, a fluorescent

probe that accumulates in mitochondria due to membrane potential, has been used to track leukocytes in numerous intravital studies, including studies of kidney (15). Figure 5A shows a field collected from a living rat injected with a closely related mitochondrial probe, rhodamine R6. Similar to the results of Heuser et al. (15) we found that rhodamine R6 labeled the circulating white cells, but also labeled endothelial cells as well, where it accumulated in peri-nuclear mitochondria (red fluorescence adjacent to elongate endothelial nuclei). As expected, mitochondrial accumulation of rhodamine R6 dissipated in an animal whose kidney had been clamped to induce ischemia (data not shown). Intravenously administered rhodamine R6 also brightly labeled mitochondria of the glomerular capillaries (data not shown), but did not label the mitochondria of renal tubule cells.

Circumventing the problems of intravenous delivery of fluorescent probes – micropuncture delivery to renal tubules and the use of GFP. While for some studies we are interested in how intravenously administered probes are transported through the kidney, frequently it is necessary to characterize a particular type of cell. As described above, we have found that intravenous administration of some probes (e.g. Hoechst 33342) is sufficient to label an array of cell types in the kidney, but intravenous injection of other probes (e.g. rhodamine R6) results in labeling of only a subset of kidney cells. Therefore, the delivery of fluorescent probes to the cells of interest is a concern for many studies of living animals.

In the case of kidney tubules, probes that would not pass the glomerular filtration barrier can be delivered to kidney tubules via micropuncture delivery (39, 42). Figure 5B shows a field collected from the kidney of a rat approximately an hour after micropuncture injection of 500 Kd MW fluorescein dextran into the lumen of a proximal tubule. In the proximal tubular segment shown here, the injected dextran had been internalized into endosomes of proximal tubule cells. As the micropuncture procedure was conducted on a separate microscope stand, finding the labeled segment

was facilitated by marking the region of the microinjected tubules with Sudan black-stained castor oil that was visible to the naked eye. The fluorescence of the stained oil can be seen in the lumens of several adjacent tubule segments.

One way of specifically labeling a particular population of cells is to utilize transgenic animals expressing GFP in a cell-specific manner. Figure 5C shows a projection of a 3-dimensional image volume collected intravitally from a mouse expressing GFP driven by the Tie-2 promotor, which is restricted to endothelial cells (26). The green fluorescence of GFP can be seen in the cytosol of the endothelia of this 50-micron-thick volume, which is better appreciated as an animated rendering located at "http://www.nephrology.iupui.edu/dunnetal". This volume also shows the same punctate brown autofluorescence seen in previous images of rat proximal tubule cells.

Expression of GFP by the leukocytes of an animal can be accomplished by transplantation with bone marrow cells expressing GFP. Figure 5D shows a microscope field collected intravitally from the kidney of a mouse that had been transplanted with bone marrow cells transduced with a retroviral vector expressing enhanced GFP (45). This mouse had also been injected with Hoechst 33342, 10 Kd MW fluorescein dextran and 500 Kd MW rhodamine dextran, which labeled cell nuclei, endosomes of the proximal tubule and the blood plasma, respectively. This image is a single frame from a 6 second series of images collected every 0.5 seconds, which is shown at "http://www.nephrology.iupui.edu/dunnetal". In this and other time series observations, many fluorescent leukocytes were detected flowing rapidly through the small vessels perfusing the renal cortex.

Discussion

The use of 2-photon microscopy for intravital studies of the kidney. When applied to living animals, optical microscopy can provide a powerful, non-invasive means of evaluating cell biology in the most physiologically relevant setting. While early studies were primarily directed at studies of blood flow and leukocyte dynamics, the ability of 2-photon microscopy to collect optical sections deep into biological tissues opened up the field of intravital microscopy to high-resolution studies of the brain, lens, skin and tumors. In each case, 2-photon microscopy provided physiological and morphological data at a spatial and temporal resolution orders of magnitude finer than that accessible through other intravital techniques such as magnetic resonance imaging or positron emission tomography. Studies of embryonic development (35) and neural development (24) indicate that 2-photon microscopy may be performed on living animals with minimal perturbation of delicate biological processes.

Here we describe studies demonstrating numerous ways that intravital 2-photon microscopy can be applied to various aspects of renal biology. Studies of animals injected with nuclear dyes may be used to assess acute effects of insults on cell necrosis and apoptosis. Studies of animals injected with bulk fluid probes may be used to evaluate blood flow, glomerular filtration and tubular transit and transport in individual segments. The kinetics of receptor-mediated endocytosis may be evaluated by injection of filtered ligands. Intravenously injected potential-sensitive dyes may be used to evaluate the energy state of individual cells. Finally, the acute behaviors of individual types of cells (e.g. inflammatory responses of endothelia and leukocytes) may be evaluated through the use of animals expressing fluorescent chimeras in specific cell types. In each case, intravital microscopy provides for

unique physiological characterizations at subcellular spatial resolution, with sub-second temporal resolution while also providing crucial information about cell-cell variability in response.

Although the titanium-sapphire laser of our system can be tuned over a range from approximately 760 nm to 920 nm, imaging is conducted with the laser tuned to a particular narrow range of wavelengths. While this might appear to limit the ability to simultaneously image more than one fluorophore using 2-photon microscopy, 2-photon excitation of commonly used fluorophores occurs over a wide range of wavelengths, and thus multiple fluorophores may be efficiently excited by a single wavelength of light (47). The ability of our 2-photon system to simultaneously collect three colors of fluorescence not only permitted the comparison of multiple probes and simultaneous characterization of multiple parameters, but was also critical to evaluating specimens with varying amounts of endogenous autofluorescence. These punctate brown-fluorescing structures, which were only found in proximal tubule cells, displayed a characteristic fluorescent spectrum that reliably distinguished them from structures labeled with introduced fluorophores.

As with any other type of fluorescence microscopy, the simultaneous excitation of multiple fluorophores results in significant "bleed-through" of signals between detector channels. While we could easily distinguish multiple probes in our implementation, in some cases this bleed-through might compromise the ability to compare the relative distributions of multiple probes. More sensitive discrimination of multiple probes can be accomplished by evaluating the emission spectrum of each pixel in an image, an approach used to distinguish two color variants of GFP (22) and to distinguish two sources of skin autofluorescence (25). Systems have recently become commercially available that combine instrumentation to collect spectroscopic image data with software designed to deconvolve the spectra into the individual fluorescence components.

The challenges of intravital 2-photon microscopy. Multi-photon microscopy provides the means to collect images of cells and tissues in living animals at sub-micron resolution. However, intravital microscopy entails various difficulties not encountered in studies of cultured cells (24).

First, animal well-being is a primary concern for any study of living animals. Animals must be properly anesthetized and maintained, for both ethical and scientific reasons. This is particularly challenging for studies in which a tissue is to be analyzed over time. In many cases surgical techniques must be developed to provide access to particular areas without compromising the tissue perfusion, innervation or function.

Second, high resolution imaging requires that the sample volume be immobilized, which for studies of living animals entails not only anesthesia, but also methods that minimize sample movement induced by respiration and the pulse during image capture. This problem is aggravated in current commercial 2-photon systems that acquire images relatively slowly. Several new high-speed 2-photon systems have been described (3, 13, 27), but these are not yet commercially available. These high-speed systems would facilitate kinetic analyses, perhaps even enabling 3-dimensional studies. While we have shown here that samples can be sufficiently immobilized to permit collections of image volumes comprising more than 80 optical sections, collection of such a volume generally takes a few minutes, which is unacceptably slow for characterizing rapid physiological events.

Third, studies of living animals are complicated by the difficulty of delivering probes to specific cells within organs. The problem of probe delivery may be avoided either by expressing fluorescent protein chimeras or by characterizing the fluorescence of endogenous molecules, some of which are environmentally sensitive and thus may be used to evaluate physiology quantitatively (1, 31).

Our studies of animals injected with bulk fluid probes demonstrate that intravenous injection is particularly useful for studies of fluid transport, where the redistribution of probes following intravenous injection provides an assay of glomerular filtration and tubular flow. The vascular route followed by fluorescent probes following intravenous injection, however, may not adequately label specific target cells. For example, we have been unable to deliver membrane-permeant probes such as rhodamine R6 and various acetoxymethyl esters (e.g. probes which could be used to measure intracellular pH and calcium concentrations) to renal tubule epithelial cells. Local delivery of these probes to tubule cells can be accomplished by tubular microinjection, which can also be used to deliver substances that are too large to pass the glomerular filtration barrier, such as large proteins, viruses, and liposomes. Thus micropuncture may be a valuable way of fluorescently labeling kidney tubules, pharmacologically manipulating single tubules and of delivering viral genetic vectors to tubular segments.

Tubular microinjection has several additional advantages over intravenous injection. Microinjection of a small amount of a drug avoids systemic effects and also limits the cost, which could be prohibitive using drug doses appropriate for the whole animal. The concentration of microinjected substances in the tubule lumen may be precisely controlled. Finally, uninjected nephrons in the same kidney provide controls for the effects of injected reagents.

A fourth issue is that the scattering of light by biological tissues limits the depth into which tissues may be imaged. As discussed above, 2-photon microscopy has extended the depth beyond that achievable by confocal microscopy so that high resolution optical sections have been collected hundreds of microns into brain tissue (11, 14, 19, 37, 38). Nonetheless, light scatter ultimately limits imaging depth of 2-photon systems as well. Since the resolution of 2-photon images is relatively unaffected by scattering (5), additional depth can be reached by simply increasing the level of

illumination (19). However, the solution of increased illumination must be approached with caution, as non-linear increases in tissue photodamage (16, 20), and disproportionate increases in photobleaching (29) are observed at higher levels of illumination. To some degree, the depth of imaging can be increased by modifying the optics of 2-photon systems to improve the efficiency of light collection, which can be optimized without regard for optical aberrations since fluorescence need not be imaged, but simply collected in 2-photon systems (28).

Future prospects for intravital 2-photon microscopy. Intravital microscopy provides a unique window into cell biology in the most meaningful context: inside living animals. The studies described here demonstrate how 2-photon microscopy can provide a level of resolution previously unattainable in intravital microscopy, enabling kinetic analyses and physiological studies in living animals with subcellular resolution. We have demonstrated the utility of 2-photon microscopy for studies of the kidney, but we have used the same general approach to image the liver, pancreas, prostate, lung and spleen. Thus 2-photon microscopy will provide a powerful tool for studying cells and tissues of a variety of organs.

Two-photon microscopy is a relatively new technique, having been first described in 1990 (9, 10) with commercial systems not available until 1996. Because of this, and the expense of commercial systems, relatively few biomedical laboratories have had access to 2-photon systems. Nonetheless, 2-photon microscopy is growing rapidly. Indeed, a literature search indicates that the number of publications using 2-photon microscopy closely fits an exponential function of time since 1993, one that predicts that the next two years will see a doubling in the total number.

Another consequence of the recency of 2-photon microscopy is that it is a relatively immature technology, particularly relative to biological imaging. The utility of 2-photon microscopy will be improved as the unique optics and photophysics of 2-photon microscopy are better understood, and

incorporated into the design of instruments and fluorescent probes. The utility of 2-photon microscopy for intravital imaging will also evolve as biomedical researchers imagine new ways to exploit this powerful technique.

Acknowledgments

This work was supported by the Indiana University Strategic Directions Initiative (K.W. Dunn), N.I.H. grant P01 DK53465 (K.W. Dunn, B. A. Molitoris, S. J. Atkinson), N.I.H. grant K08 DK02634 (K. J. Kelly) and a grant (InGen) from the Lilly Foundation to the Indiana University School of Medicine (B. A. Molitoris). We thank M.C. Dinauer, A. Yamauchi and N. Pesch for providing the mouse transplanted with GFP-expressing bone marrow cells. We would also like to gratefully acknowledge the technical assistance of Sarafina K. Salamo.

BIBLIOGRAPHY

1. Bennett B, Jetton T, Ying G, Magnuson M, Piston DW. Quantitative subcellular imaging of glucose metabolism within intact pancreatic islets. *J. Biol. Chem*. 271:3647-3651, 1996.
2. Brown BE, Campbell RB, Yoshikazu T, Lei X, Carmeliet P, Rakesh KJ. *In vivo* measurement of gene expression, angiogenesis and physiological function in tumors using multiphoton laser scanning microscopy. *Nature Medicine* 7:864-868, 2001.
3. Buehler C, Kim K, Dong C, Masters B, So P. Innovations in two-photon deep tissue microscopy. *IEEE Engineering in Med. Biol.* 18:23-30, 1999.
4. Buhrle C, Hackenthal E, Helmchen U, Lackner K, Nobiling R, Steinhausen M, Taugner R. The hydronephrotic kidney of the mouse as a tool for intravital microscopy and in vitro electrophysiological studies of renin-containing cells. *Lab. Invest*. 54:462-472, 1986.
5. Centonze V, White J. Multiphoton excitation provides optical sections from deeper within scattering specimens than confocal imaging. *Biophys. J.* 75:2015-2024, 1998.
6. Chen B, Lendvai B, Nimchinsky E, Burbach B, Fox K, Svoboda K. Imaging high-resolution structure of GFP-expressing neurons in neocortex in vivo. *Learn. Memory*. 7:433-441, 2000.
7. Clendenon JL, Phillips CL, Sandoval RM, Fang S, Dunn K.W. Voxx: A PC-based, near real-time volume rendering system for biological microscopy. *Am. J. Physiol. Cell Physiol*, 282:C213-218, 2002.
8. Clemens M, Zhang J. Regulation of sinusoidal perfusion: in vivo methodology and control by endothelins. *Sem. Liver Dis.* 19:383-396, 1999.
9. Denk W, Strickler J, Webb WW. Two-photon laser scanning fluorescence microscopy. *Science* 248:73-76, 1990.

10. Denk W, Piston DW, Webb WW 1995. Two-photon molecular excitation in laser-scanning microscopy. Handbook of Biological Confocal Microscopy, 2nd Edition. J.B. Pawley, Ed. Plenum, New York. p. 445-458, 1995.

11. Denk W, Delaney K, Gelperin A, Kleinfeld D, Strowbridge B, Tank D, Yuste R. Anatomical and functional imaging of neurons using 2-photon laser scanning confocal microscopy. *J. Neurosci. Meth* 54:151-162, 1994.

12. DeVriese A, Endlich K, Elger M, Lamiere N, Atkins R, Lan H, Rupin A, Kriz W, Steinhausen M. The role of selectins in glomerular leukocyte recruitment in rat anti-glomerular basement membrane glomerulonephritis. *J. Am. Soc. Neph*. 10: 2510-2517, 1999.

13. Fan G, Fujisake H, Miyawaki A, Tsay RK, Tsien R, Ellisman M Video-rate scanning two-photon excitation fluorescence microscopy and ratio imaging with cameleons. *Biophys J* 76:2412-2420, 1999.

14. Helmchen F, Svoboda K, Denk W, Tank D. In vivo dendritic calcium dynamics in deep-layer cortical pyramidal neurons. *Nature Neuro*. 2:989-996, 1999.

15. Heuser M, Seseke F, Zoller G, Gross A, Kugler A, Stojanovoc T, Hemmerlein B. Differences in cortical microcirculation in the kidneys of unilaterally congenital hydronephrotic rats. *Microvasc. Res.* 62: 172-178, 2001.

16. Hopt A, Heher E. Highly nonlinear photodamage in two-photon fluorescence microscopy. *Biophys. J.* 80:2029-2036, 2001.

17. Hudetz A. Blood flow in the cerebral capillary network: a review emphasizing observations with intravital microscopy. *Microcirculation* 4:233-252, 1997.

18. Kelly KJ, Plotkin Z Dagher PC. Guanosine suppplementation reduces apoptosis and protects renal function in the setting of ischemic injury. *J. Clin. Invest.* 108:1291-1298, 2001.

19. Kleinfeld D, Mitra P, Helmchen F, Denk W. Fluctuations and stimulus-induced changes in blood flow observed in individual capillaries in layers 2 through 4 of rat neocortex. *Proc Natl Acad Sci USA* 95:15741-15746, 1998.

20. Koester JH, Baur D, Ulh R, Hell SW. Ca2+ fluorescence imaging with pico- and femtosecond two-photon excitation: signal and photodamage. *Biophys. J.* 77: 2226-2236, 1999.

21. Lansford R, Bearman G, Fraser S. Resolution of multiple green fluorescent protein color variants and dyes using two-photon microscopy and imaging spectroscopy. *J. Biomed. Optics* 6:311-318, 2001.

22. Lencer, W., Weyer, P., Verkman, A., Ausiello, D. and D. Brown. 1990. FITC-dextran as a probe for endosome function and localization in kidney. Am. J. Physiol. 258:C309-C317

23. Lendvai B, Stern E, Chen B, Svoboda K. Experience-dependent plasticity of dendritic spines in the developing rat barrel cortex in vivo. *Nature* 404:876-881, 2000.

24. Lichtman J, Fraser S. The neuronal naturalist: watching neurons in their native habitat. *Nature Neuro*. 4:1215-1220, 2001.

25. Masters B, So P, Gratton E. Multiphoton excitation fluorescence microscopy and spectroscopy of in vivo human skin. *Biophys. J.* 72:2405-2412, 1997.

26. Motoike T, Loughna, S, Perens E, Roman BL, Liao W, Chau TC, Richardson CD, Kawate T, Kuno J, Weinstein BM, Stainier DYR, Sato TN. Universal GFP Reporter for the Study of Vascular Development. *Genesis* 28:75-81, 2000.

27. Nguyen QT, Callamaras N, Hsieh C, Parker I. Construction of a two-photon microscope for video-rate Ca2+ imaging. *Cell Calcium* 30:383-393, 2001.

28. Oheim M, Beaurepaire E, Chaigneau E, Mertz J, Charpak S. Two-photon microscopy in brain tissue: parameters influencing imaging depth. *J. Neurosci. Methods*. 111: 29-37, 2001.

29. Patterson G, Piston D. Photobleaching in two-photon microscopy. *Biophys. J.* 78:2159-2162, 2000.

30. Phillips C, Arend L, Kojetin D, Filson A, Clendenon J, Fang S, Dunn KW. 3-D imaging of embryonic mouse kidney by 2-photon microscopy. *Am. J. Pathol.* 158:49-55, 2001.

31. Piston DW, Masters B, Webb WW. 3-dimensional resolved NAD(P)H cellular metabolic redox imaging of the in situ cornea with 2-photon excitation laser scanning microscopy. *J Microscopy* 178:20-27, 1995.

32. Sandoval RM, Dunn KW, Molitoris BA. Aminoglycosides traffic rapidly and directly to the Golgi complex in LLC-PK1 cells. *Am. J. Physiol Renal Physiol.* 279:F884-890, 2000.

33. Sandoval RM, Leiser JD, Molitoris BA. Aminoglycoside antibiotics traffic to the Golgi Complex in LLC-PK1 cells. *J. Am. Soc. Nephro.l* 9:167-174, 1998.

34. Schafer K, Gretz N, Bader M, Oberbaumer I, Eckardt KU, Kriz W, Bachmann S. Characterization of the Han:SPRD rat model for hereditary polycystic kidney disease. *Kidney Int* 46:134-152, 1994.

35. Squirrell J, Wokosin D, White J, Bavister B. Long-term two-photon fluorescence imaging of mammalian embryos without compromising viability. *Nature Biotech.* 17:763-767, 1999.

36. Steinhausen M, Muller P, Parekh N. Renal test dyes IV. Intravital fluorescence microscopy and microphotometry of the tubularly secreted dye sulfonefluorescein. *Pfluegers Arch Eur J Physiol* 364:83-89, 1976.

37. Svoboda K, Tank D, Denk W. Direct measurement of coupling between dendritic spines and shafts. *Science* 272:716-719, 1996.

38. Svoboda K, Denk W, Kleinfled D, Tank D. In vivo dendritic calcium dynamics in neocortical pyramidal neurons. *Nature* 385:161-165, 1997.

39. Tanner GA. Nephron obstruction and tubuloglomerular feedback. *Kidney Int* 22:213-218, 1982.

40. Tanner GA, Gretz N, Shao Y, Evan A, Steinhausen M. Organic anion secretion in polycystic kidney disease. *J. Am. Soc. Nephrol.* 8:1222-1231, 1997.

41. Tanner GA, Steinhausen M. Tubular obstruction in ischemia-induced acute renal failure in the rat. *Kidney Int.* 6:S65-73, 1976.

42. Tanner GA, Knopp L. Glomerular blood flow after single nephron obstruction in the rat kidney. *Am J Physiol Renal Physiol.* 250:F77-F85, 1986.

43. Uhlmann S, Uhlmann D, Spiegel H. Evaluation of hepatic microcirculation by in vivo microscopy. *J. Invest. Surg.* 12:179-193, 1999.

44. Vajkoczy P, Ullrich A, Menger M. Intravital fluorescence microscopy to study tumor angiogenesis and microcirculation. *Neoplasia* 2:53-61, 2000.

45. Williams DA, Tao W, Yang F, Kim C, Gu Y, Mansfield P, Levine JE, Petryniak B, Derrow CW, Harris C, Jia B, Zheng Y, Ambruso DR, Lowe JB, Atkinson SJ, Dinauer MC, Boxer L. Dominant negative mutation of the hematopoietic-specific Rho GTPase, Rac2, is associated with a human phagocyte immunodeficiency. *Blood* 96:1646-1654, 2000.

46. Winet H. The role of microvasculature in normal and perturbed bone healing as revealed by intravital microscopy. *Bone* 19:39S-57S, 1996.

47. Xu C, Williams R, Zipfel W, Webb WW. Multiphoton excitation cross-sections of molecular fluorophores. *Bioimaging* 4:198-207, 1996.

Table 1. Fluorescent probes used in these studies.

PROBE	LOCALIZATION	QUANTITY (rat/mouse)
Hoechst 33342	Membrane permeant DNA-binding probe. Intravenous injection labels nuclei of all cells of kidney	500 μg/250 μg
Propidium iodide	Membrane impermeant DNA-binding probe, labels nuclei of apoptotic and necrotic cells. Accessible to all cells of kidney after intravenous injection.	10 μg/not applicable
10,000 MW Dextran	Bulk fluid-phase marker that is freely filtered by the glomerulus following intravenous injection. Briefly found in vasculature, rapidly filtered into renal tubules. Internalized into endosomes of proximal tubule where it accumulates in lysosomes.	3 mg/600 μg
500,000 MW Dextran	Bulk fluid-phase marker that is retained in the vasculature of animals with intact glomerulus following intravenous injection.	400 μg /100 μg
Bovine serum albumin	Bulk fluid-phase marker that is retained in the vasculature of animals with intact glomeruli following intravenous injection.	2 mg/not applicable
Texas Red Gentamicin	Small molecular weight therapeutic antibiotic that is freely filtered across the glomerulus following intravenous injection. It is internalized into endosomes of proximal tubule cells where it then accumulates in lysosomes.	2 mg/not applicable
Rhodamine R6	Vital probe that accumulates in active mitochondria on the basis of membrane potential. Intravenous injection results in labeling of endothelia and circulating white cells.	2 μg/not applicable

Figure 1. Diagram of experimental setup used for intra-vital imaging of live rodent kidneys. Animals were anaesthetized and prepared as described in Methods and then placed on the stage of an inverted microscope with the exposed kidney placed in a 50mm coverslip-bottomed cell culture dish bathed in normal saline. The heating pad was then placed directly over the animal. Imaging was conducted using a Nikon 60X N.A. 1.2 water immersion objective.

Figure 1

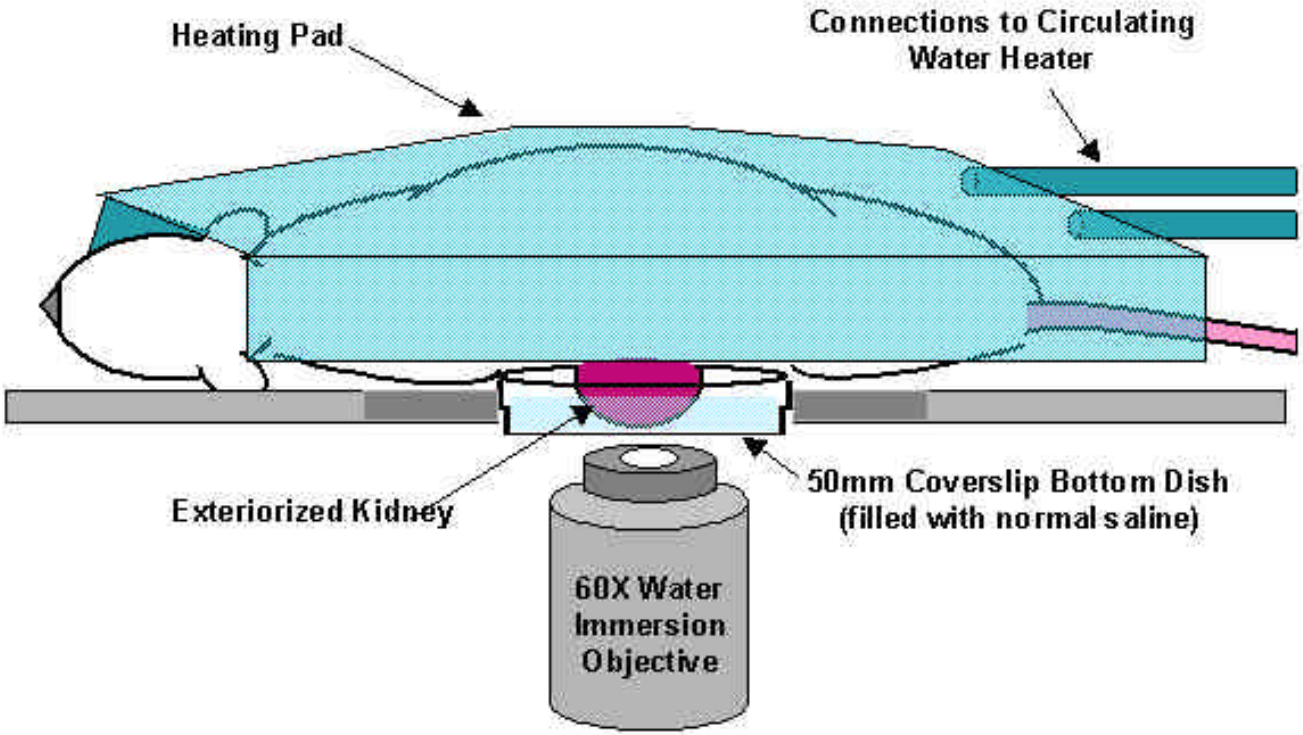
Heating Pad
Connections to Circulating Water Heater
Exteriorized Kidney
50mm Coverslip Bottom Dish (filled with normal saline)
60X Water Immersion Objective

Figure 2. DNA stains can be used as intravital labels of cell nuclei in the kidney and to identify necrotic or apoptotic cells. (**A** & **B**) Projections of image volumes (each approximately 50 microns thick) from the superficial cortex of rat kidneys. The volume shown in panel (A) was collected from a normal rat injected with propidium iodide and Hoechst 33342. The volume shown in panel (B) is similar, except that it was collected from a rat subjected to 30 minutes of unilateral renal ischemia produced by renal pedicle clamping. After 24 hr of recovery, propidium iodide and Hoechst 33342 were injected i.v. Necrotic and apoptotic nuclei in the ischemic kidney appear white (arrows), due to the combination of Hoechst and propidium iodide fluorescence. Note that these volumes are better appreciated as Voxx-rendered animations that may be downloaded at "http://www.nephrology.iupui.edu/dunnetal". (**C** & **D**) Single focal plane images collected from the kidney of a rat subjected to brief (30 min) ischemia with 24 hr recovery. Whereas the image of the cortex (C) shows little evidence of cell death, numerous dead cells are apparent in the image of the outer medulla (D). As described in the text, large arrows indicate nuclei of necrotic cells, small arrows indicate the condensed nuclei of cells at early stages of apoptosis and arrowheads indicate the nuclei of cells at later stages of apoptosis, whose labeling with propidium iodide reflects secondary necrosis. The medullary region was examined in an animal after preparation of a parenchymal window. The scale bar is 40 microns in length.

Figure 2

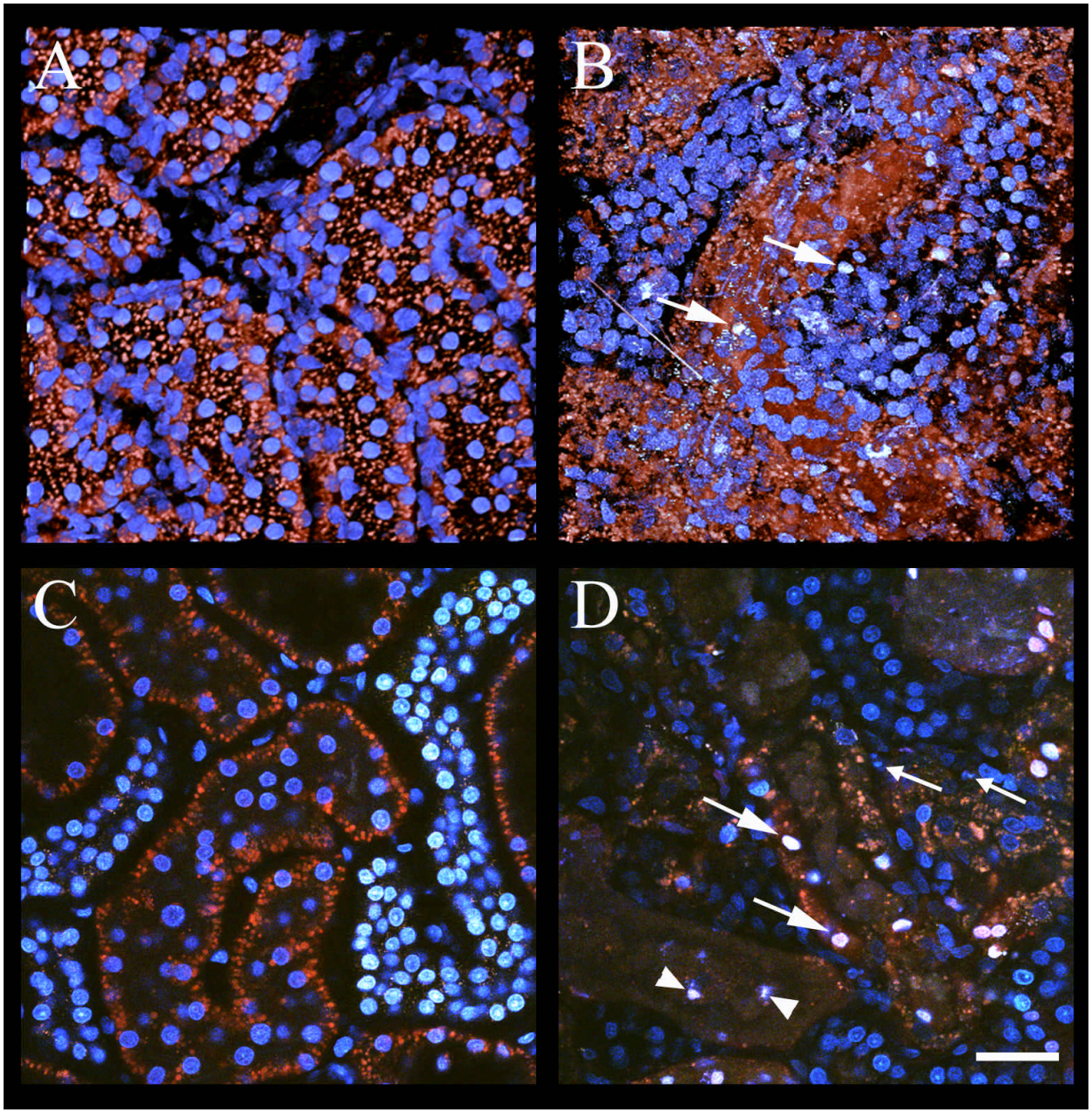

Figure 3. Bulk fluid-phase probes can be used to evaluate renal fluid dynamics intravitally. (**A**) Image collected from a living rat that had been injected with Hoechst 33342, rhodamine-conjugated albumin and 10,000 MW fluorescein-conjugated dextran. The 20 second time series from which this panel was obtained is shown at "http://www.nephrology.iupui.edu/dunnetal". In the cross section shown in this field, intertubular capillaries (containing red-fluorescing albumin) are seen running between proximal tubule segments (containing punctate green fluorescence of fluorescein-dextran internalized into endosomes) and distal tubules (which lack endosomal dextran, but show lumenal accumulation, bottom right). (**B**) Image collected at the level of the glomerulus from a living Munich-Wistar rat that had been injected with Hoechst 33342 and a 500,000 MW fluorescein conjugated dextran. The 30 second time series, from which this image was selected is shown at "http://www.nephrology.iupui.edu/dunnetal". In this time-series, blood flow through the glomerulus is apparent from the shadows of circulating cells moving in the green-fluorescing volume of the blood. (**C**) Image collected from the kidney of a living rat 14 minutes after injection of Hoechst 33342, 500,000 MW fluorescein conjugated dextran and 10,000 MW rhodamine dextran. A similar field, collected after another 11 minutes, is shown in Panel (**D**). In these, and the following field, the green fluorescence of fluorescein dextran labels the peritubular capillaries running between proximal tubule segments (containing punctate red fluorescence of endosomal rhodamine dextran) and distal tubules (which lack endosomal uptake, but show a lumenal accumulation of rhodamine dextran). (**E**) Mouse kidney image following injection with 500,000 MW fluorescein conjugated dextran and 10,000 MW rhodamine dextran. (**F**) Projection of a 90 micron deep image volume collected from the kidney of a living heterozygous Han:SPRD rat with polycystic kidney disease following intravenous injection with Hoechst 33342 and 10,000 MW rhodamine dextran. This volume is also presented as an animated rendering at "http://www.nephrology.iupui.edu/dunnetal". The scale bar is 40 microns in length.

Figure 3

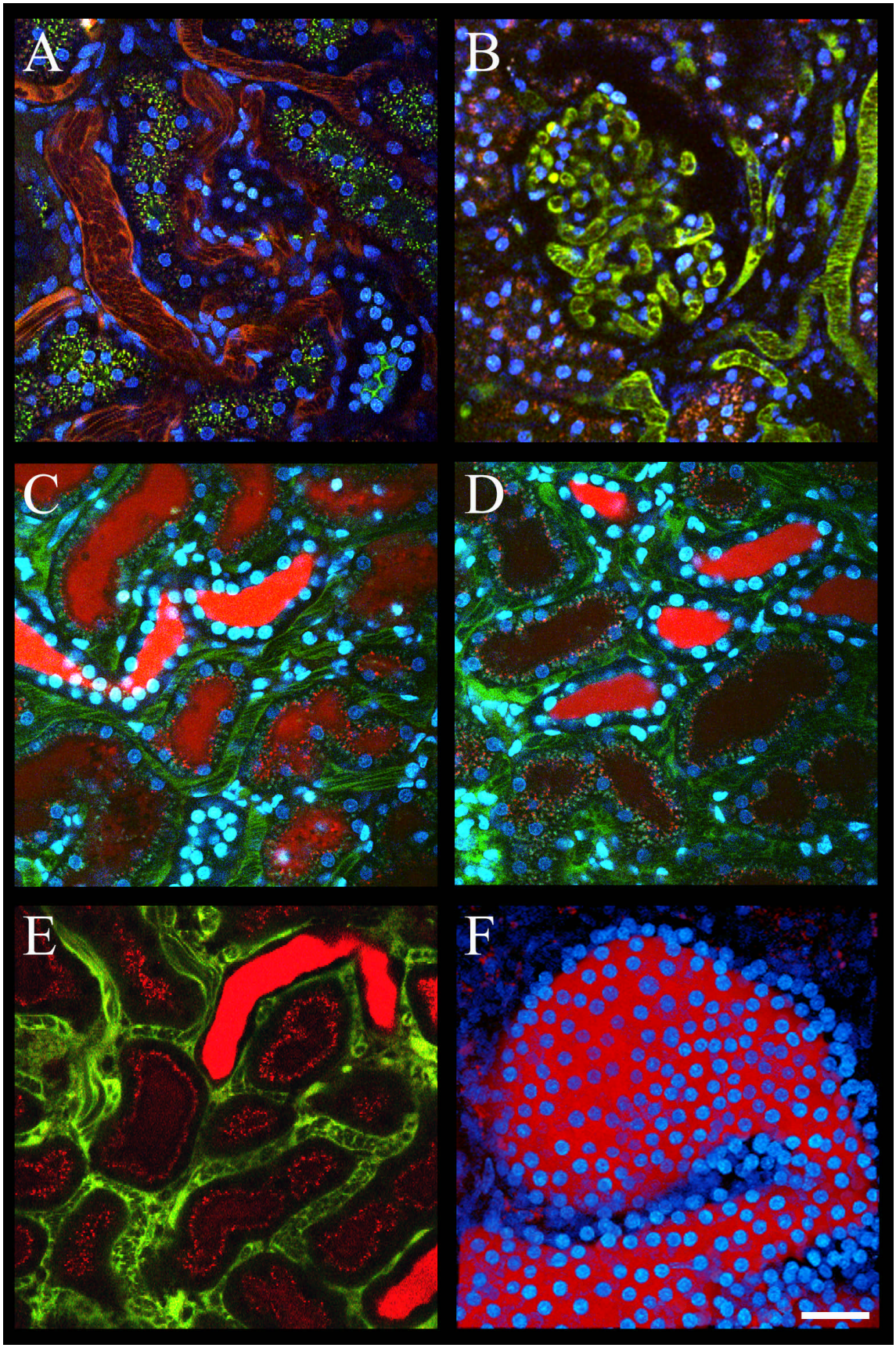

Figure 4. Time series of Texas Red gentamicin transport in the intact rat kidney. (**A**) High magnification image of a kidney of a rat collected intravitally 11 minutes following intravenous injection of Texas Red-conjugated gentamicin into the tail vein. Gentamicin can be seen dimly labeling the lumen of the proximal tubule at the center of the field, and brightly labeling endosomes where it has accumulated (arrows). Arrowheads indicate punctate brown autofluorescent structures at the base of proximal tubule cells. (**B**) A microscope field collected within 1 minute of injection of Texas Red gentamicin, showing strong labeling of peritubular capillaries running between the tubular segments, as well as the lumen of proximal tubules (identified by their distinctive punctate brown autofluorescence). (**C**) A field collected within 3 minutes of injection, showing that gentamicin has been largely cleared from the blood and from the proximal tubule, and has reached the lumen of two distal tubule segments at the top of the field. (**D**) The same field collected one minute later, during which time the bolus of gentamicin has begun to clear the distal tubule segments previously labeled, and has now reached new segments at the bottom and right side of the field. The scale bar reflects a length of 40 microns except for panel A, where it reflects a length of 13 microns.

Figure 4

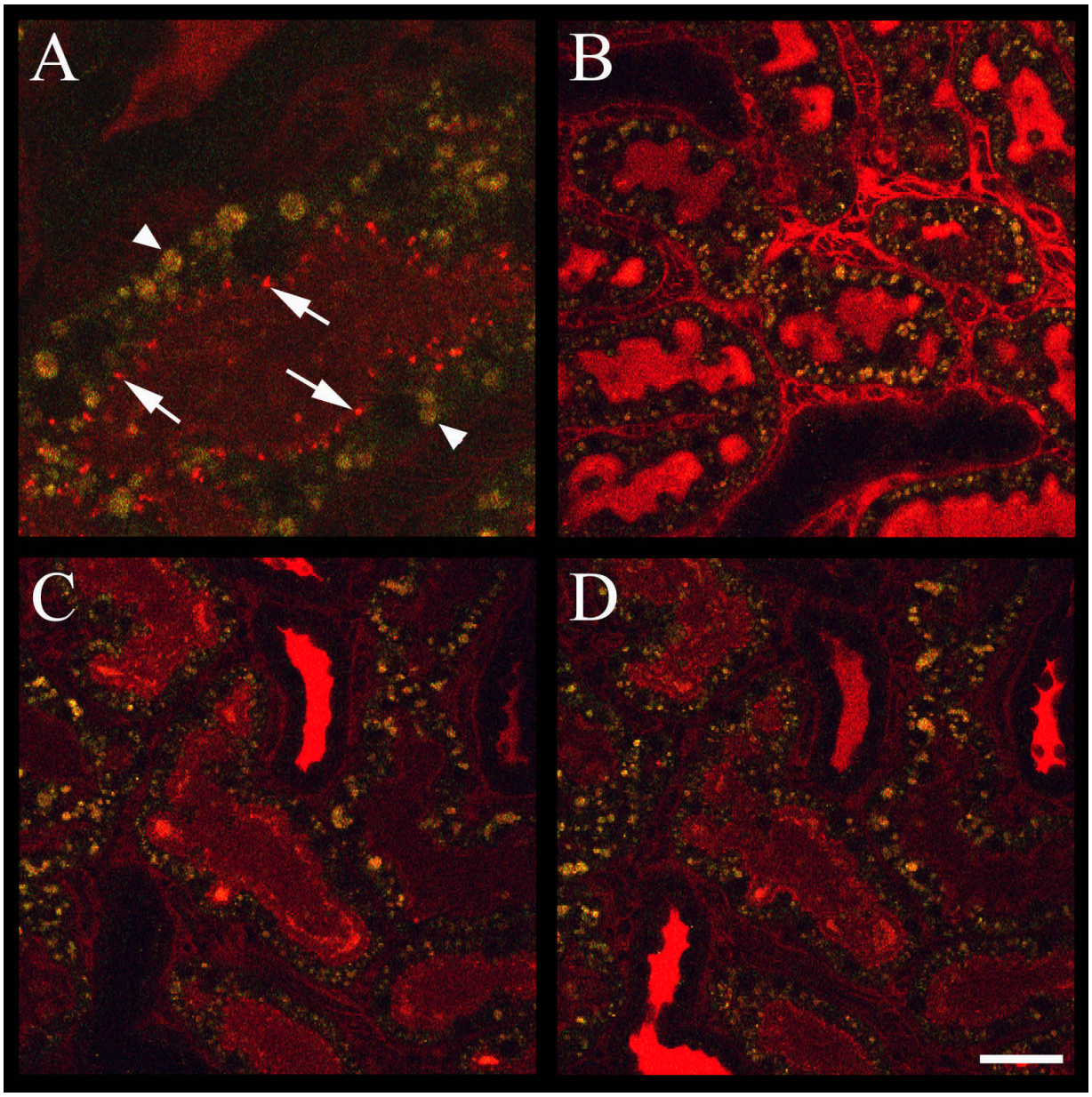

Figure 5. Intravital fluorescence microscopy using potential-sensitive mitochondrial dyes, and expression of GFP. (**A**) An image of the kidney of a living rat following intravenous injection of rhodamine R6 and Hoechst 33342 shows accumulation of rhodamine R6 in mitochondria of endothelial cells (arrows). Note that the red fluorescence of rhodamine R6 in endothelial cells can be clearly distinguished from the brown autofluorescent inclusions of the adjacent proximal tubule cells. (**B**) An image of the kidney of a rat following micropuncture delivery of 500 Kd fluorescein dextran into the lumen of proximal tubule. In addition to the fluorescein dextran fluorescence in the endosomes of proximal tubule cells, the field also shows several tubular lumens with the orange fluorescence of the Sudan black-stained castor oil used to locate microinjected tubules. (**C**) Projection of a three-dimensional volume collected from the kidney of a living transgenic mouse expressing GFP driven by an endothelial-specific promotor (Tie-2). The microvasculature, as delineated by the GFP expressing endothelial cells, is seen surrounding renal cortical proximal tubules that, as in rats, contain brown autofluorescent inclusions. This volume is also presented as an animated rendering at "http://www.nephrology.iupui.edu/dunnetal". (**D**) An image of the kidney of a mouse transplanted with bone marrow cells expressing enhanced GFP. This panel is a single frame from a time series of images collected every 0.5 seconds showing the rapid movement of leukocytes through peritubular capillaries. The arrow indicates one such leukocyte. This mouse had also been injected with Hoechst 33342, 500 Kd rhodamine dextran and 10 Kd fluorescein dextran. Note that the 500 Kd rhodamine dextran was not sufficiently dialyzed for this study, consequently small molecular weight components apparently present in this probe were filtered through the glomeruli into tubules. Scale bar reflects a length of 25 microns in panel A, 50 microns in panel B and 40 microns in panels C and D.

Figure 5